Investigation of a Neat versus Magnetically Diluted Powdered Mononuclear Mn^{II} Complex by High-Field and High-Frequency EPR Spectroscopy

Claire Mantel,[a,b] Christian Philouze,[c] Marie-Noëlle Collomb,*[b] and Carole Duboc*[a]

Keywords: Azide ligand / Electronic structure / EPR spectroscopy / Manganese / Magnetic dilution

The isolation, structural characterization and electronic properties of a new mononuclear, pentacoordinate Mn^{II} complex [Mn(*t*Buterpy)$(N_3)_2$] (**1**; *t*Buterpy = 4,4′,4′′-tri-*tert*-butyl-2,2′:6′,2′′-terpyridine) is reported. The X-ray structure of **1** reveals that the manganese ion lies in the center of a distorted trigonal bipyramid. The electronic properties of **1** were investigated by high-field and high-frequency EPR (HF-EPR) spectroscopy, allowing the determination of the spin-Hamiltonian parameters. HF-EPR spectra were recorded on a neat powder of **1** and also on **1** magnetically diluted in the corresponding zinc complex. From the neat powder HF-EPR spectra, the following *g* and zero-field-splitting terms, as well as the sign of *D*, were obtained: $D = -0.250(5)$ cm^{-1}, $E = 0.044(5)$ cm^{-1} and $g_x = g_y = g_z = 2.000(5)$. The magnetically diluted sample allows the determination of the hyperfine coupling constant *A* and confirms the values of the parameters determined with the neat powder: $|D| = 0.260(1)$ cm^{-1}, $E = 0.043(1)$ cm^{-1}, $g_x = g_y = 2.001(1)$ $g_z = 2.0005(5)$ and $A_{xx} = A_{yy} = A_{zz} = 77.5(5)$ G. A comparison between these two sets of spin-Hamiltonian parameters is discussed, as well as the correlation between the *D* parameter and the coordination number around the manganese ion for a coordination shell characterized by O and/or N atoms (i.e. Mn^{II}-containing proteins).

Introduction

Mononuclear Mn^{II} complexes are present in several metalloproteins implicated in various important biological processes. Examples include manganese superoxide dismutase, an antioxidant enzyme that catalyzes the dismutation of the superoxide radical,[1] concanavaline A, a saccharide-binding protein,[2] the fosfomycin resistance protein implicated in the resistance against the antibiotic fosfomycin,[3] and several others.[4] Since the manganese site is essential for their activity, a precise determination of the geometry and the coordination shell of the metallic ion is required to understand the reactivity of these proteins. One of the best techniques used to elucidate the electronic structure of a metallic center is EPR spectroscopy. In particular, X-band EPR spectroscopy (9.4 GHz) has been used to study several biological Mn^{II} sites.[1b−1d,2c,2d,3,4]

High-spin Mn^{II} ($3d^5$) is characterized by a fundamental electronic spin *S* of 5/2 and a nuclear spin *I* also of 5/2 (^{55}Mn, 100%). Its electronic properties are described by the spin-Hamiltonian of Equation (1).

$$H = \beta B \cdot g \cdot S + I \cdot A \cdot S + D[S_z^2 - 1/3S(S+1)] + E(S_x^2 - S_y^2) \quad (1)$$

The first two terms represent the electronic Zeeman and the electron nuclear hyperfine interactions, respectively, whereas the last two terms define the zero-field splitting (zfs) interaction, with *D* and *E* weighting the axial and rhombic parts.

A typical Mn^{II} EPR spectrum for mononuclear complexes with small zfs parameters, recorded under highly diluted conditions (in solution) and at high temperature, is characterized by a unique feature centered at $g \approx 2.0$ as a sextuplet. These six lines originate from the hyperfine splitting of the central transition $|5/2, -1/2> \rightarrow |5/2, +1/2>$, as shown in Figure 1. The shape of the sextuplet depends on the magnitude of the different spin-Hamiltonian terms. When the zfs terms increase, the X-band EPR spectrum becomes increasingly more complicated and almost impossible to interpret, with broad transitions between 0 and 0.5 mT. In this case, the way to simplify the Mn^{II} EPR spectra is to record them at higher microwave frequencies such as 35 GHz (Q-band EPR), 95 GHz or even up to 285 GHz

[a] Grenoble High Magnetic Field Laboratory, Laboratoire des Champs Magnétiques Intenses, CNRS UPR 5021, MPI
B. P. 166, 38042 Grenoble Cedex 9, France
Fax: (internat.) + 33-4-76855610
E-mail: duboc@grenoble.cnrs.fr
[b] Laboratoire d'Electrochimie Organique et de Photochimie Redox, Université Joseph Fourier, CNRS UMR 5630, Institut de Chimie Moléculaire de Grenoble (ICMG), FR CNRS 2607
B. P. 53, 38041 Grenoble cedex 9, France
Fax: (internat.) + 33-4-76514267
E-mail: Marie-Noelle.Collomb@ujf-grenoble.fr
[c] Laboratoire d'Etudes Dynamiques et Structurales de la Sélectivité, Université Joseph Fourier, CNRS UMR 5616, ICMG, FR CNRS 2607
B. P. 53, 38041 Grenoble cedex 9, France

  DOI: 10.1002/ejic.200400325

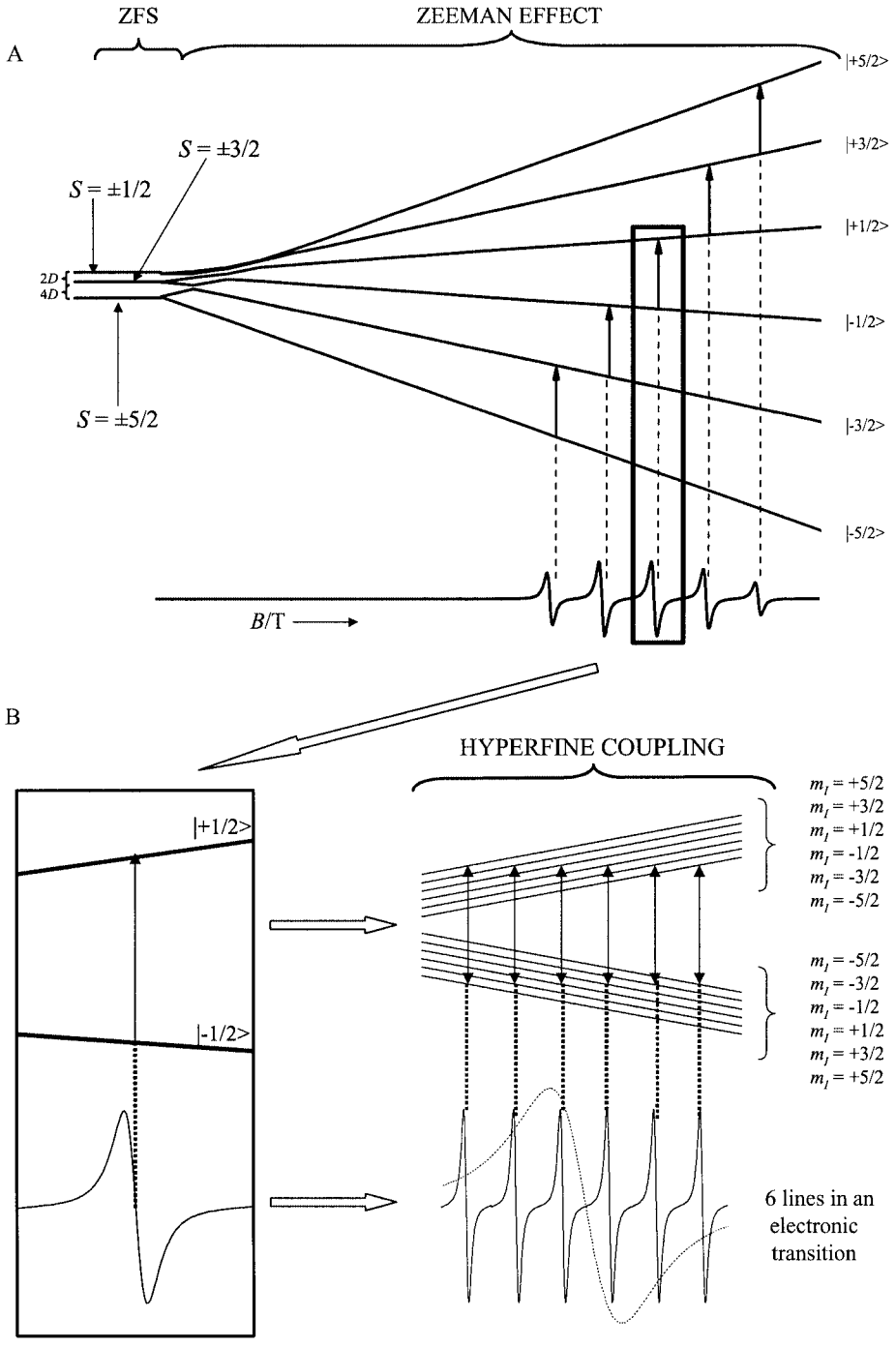

Figure 1. (A) Schematic representation of the energy level diagram of an $S = 5/2$ system undergoing axial zero field splitting (zfs) (negative D) and Zeeman effect with the field parallel to the z axis; (B) extended view of the $Ms = \pm 1/2$ energy levels showing the hyperfine levels for $I = 5/2$; arrows indicate the allowed transitions and the resulting spectra are given

(high-field EPR, HF-EPR). Indeed, HF-EPR spectroscopy (frequency 95 GHz) and derived techniques such as high-field ENDOR have proven to be useful tools.[1d,1e,2d,5] Under high-field conditions ($D << g\beta B$), EPR spectra recorded on an Mn^{II}-containing protein solution exhibit a simplified sextuplet from which the spin-Hamiltonian parameters can be extracted. However, when the magnitude of D is very large ($|D| > 0.2$ cm^{-1}), even at high field (285 GHz, $g = 2$ at 10.2 T), the central transition $|5/2, -1/2> \rightarrow |5/2, +1/2>$ appears as a signal characterized by more than six lines.[1d,1e] With such Mn^{II} systems, a multi-frequency HF-EPR study is necessary for a precise determination of the spin-Hamiltonian parameters.

Concerning the other transitions of the paramagnet $S = 5/2$ displayed in Figure 1, four others are expected along each magnetic axis. However, they are rarely observed and studied by X-band EPR spectroscopy, especially when the experiments are performed in solution.

X- and Q-band EPR studies performed on powdered or crystalline samples of synthetic mononuclear Mn^{II} complexes have also been reported.[6] The analysis of the EPR spectra is feasible for systems with small *D* values due to the observation of some or all expected transitions. Nevertheless, Mn^{II} complexes are often characterized by relatively large axial zfs, and when *D* is larger than or similar to the energy provided by the EPR spectrometer, the spectra become more complicated and not interpretable. Furthermore, with neat powder samples the hyperfine interactions cannot be observed. In order to detect them, the manganese complexes need to be diluted into a diamagnetic host. In the few studies related to magnetic dilution,[7] the X- or Q-band EPR spectra show several transitions split by hyperfine interactions that can help with the determination of the spin-Hamiltonian parameters when *D* is relatively large.

Another way to obtain interpretable spectra of manganese(II) complexes with large *D* values is the use of HF-EPR spectroscopy. In this case, with neat powder samples more, or even all, transitions can be then observed than with X-band, allowing the precise determination of the spin-Hamiltonian parameters. To the best of our knowledge, only two HF-EPR studies, showing complete or quasi-complete EPR spectra of Mn^{II} complexes, have been reported so far.[8] The compounds were three series of synthetic mononuclear dihalo complexes with distorted octahedral[8a] or tetrahedral[8b] geometries. The HF-EPR experiments were carried out on neat powder samples at 94.5 and 250 GHz avoiding the observation of hyperfine splitting in the different electronic-spin transitions. The spin-Hamiltonian parameters were determined, although the sign of *D* was not extracted since the experiments were performed at room temperature.

In this paper, we report the synthesis, the crystallographic characterization and an HF-EPR study (190−285 GHz) of a new synthetic pentacoordinate inorganic complex: [Mn(*t*Buterpy)$(N_3)_2$] (**1**; *t*Buterpy = 4,4′,4′′-tri-*tert*-butyl-2,2′:6′,2′′-terpyridine). The EPR experiments were performed both on a neat powder of **1** and on the complex diluted into the corresponding zinc(II) complex, [Zn(Mn)(*t*Buterpy)$(N_3)_2$]. We chose this solid magnetic dilution rather than a dilution of **1** in a solvent in order to maintain the pentacoordination of **1**. This work allows us to compare the spin-Hamiltonian parameters obtained in both conditions (neat and magnetically diluted samples of **1**). We can thus discuss the validity of the approach developed for several Mn^{II} protein EPR studies in which only the sextuplet is used to determine the electronic structure of the Mn^{II} site.

Results

Description of the Crystal Structure of [Mn(*t*Buterpy)$(N_3)_2$] (1)

The crystal structure of complex **1** was determined by single-crystal X-ray crystallography and its structure is shown in Figure 2.[9] The principal crystallographic data are given in the Exp. Sect., while Table 1 summarizes selected bond lengths and angles.

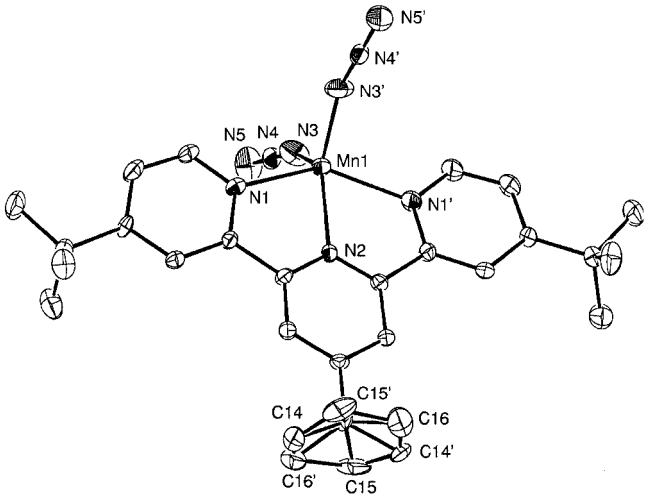

Figure 2. ORTEP view of [Mn(*t*Buterpy)$(N_3)_2$]; hydrogen atoms have been omitted for clarity

Table 1. Selected bond lengths [Å] and angles [°] for complex **1**

Mn−N(1)	2.249(5)	N(1)−Mn−N(1′)	144.1(2)
Mn−N(2)	2.206(5)	N(1)−Mn−N(3)	101.0(2)
Mn−N(3)	2.038(5)	N(1)−Mn−N(3′)	99.6(2)
N(1)−Mn−N(2)	72.0(1)	N(3)−Mn−N(3′)	108.8(3)
N(2)−Mn−N(3)	125.6(2)		

The manganese ion lies in the center of a distorted trigonal bipyramid. The equatorial plane is occupied by two nitrogen atoms of the two azide ligands [N(3) and N(3′)] and the central nitrogen atom [N(2)] of *t*Buterpy. The two distal *t*Buterpy nitrogen atoms [N(1) and N(1′)] are in the axial positions. The structure possesses a rotational C_2 symmetry axis passing through the Mn and N(2), atoms implying that the atoms N(3) and N(3′) are crystallographically equivalent, as are N(1) and N(1′). It can also be seen that the *tert*-butyl group of the central pyridine ring rotates around this C_2 axis. This implies that each carbon atom of the *tert*-butyl group [C(14), C(15) and C(16)] possesses two equivalent crystallographic sites whose occupancy ratio is 50%. The $Mn-N_{tButerpy}$ bond lengths and the angles N(1)−Mn−N(1′) and N(1)−Mn−N(2) are typical for mononuclear (terpy)Mn^{II} complexes.[10] The Mn−N(2) distance [2.206(5) Å] is shorter than the Mn−N(1) distance [2.249(5) Å].[10] The magnitude of the N(1)−Mn−N(1′) [144.1(2)°] is reduced from the theoretical value of 180° of an idealized trigonal bipyramid due to the rigidity of the *t*Buterpy ligand. The angles between the atoms in the equatorial positions are 125.6(2)° [N(2)−Mn−N(3){N(3′)}] and 108.8(3)° [N(3)−Mn−N(3′)]. These values are a measure of the distortion as a value of 120° is expected for an undistorted trigonal bipyramid. The $Mn-N_{azide}$ bonds [2.038(5)

Å] in **1** are slightly shorter than those observed in $[Mn(phen)_2(N_3)(H_2O)]^+$ (2.151 Å) or $[Mn(phen)_2(N_3)_2]$ (av. 2.138 Å) (phen: 1,10-phenanthroline).[11]

HF-EPR Spectroscopy of a Neat Powder of [Mn(*t*Buterpy)-$(N_3)_2$]

The electronic properties of a neat powder sample of complex **1** were investigated by a multi-frequency EPR study between 190 and 285 GHz and over a temperature range of 5−30 K. Figure 3 shows experimental and simulated 285 GHz HF-EPR spectra recorded at 5 and 10 K. At this frequency, the spectra show transitions located between 9.0 and 11.2 T. Since high-field limit conditions are reached ($D << g\beta B$), all of the transitions are allowed, permitting an easy interpretation of the experimental data.

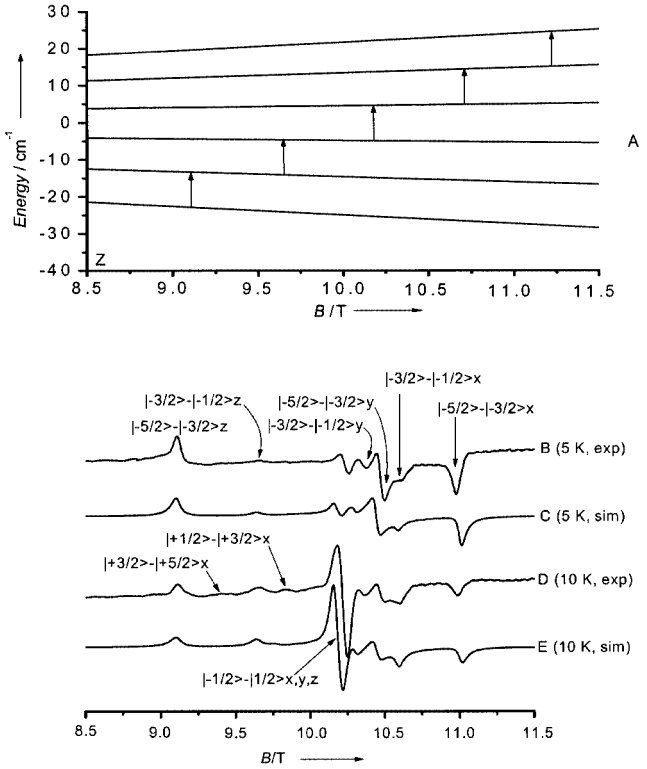

Figure 3. Plots of energy vs. field for the six levels arising from an $S = 5/2$ spin state using the parameters given below; the field is parallel to the molecular z axis (A); arrows indicate the observed resonances; experimental (B and D) and simulated (C and E) powder 285 GHz EPR spectra of **1**, recorded at 5 K (B and C) and 10 K (D and E); the parameters used for the simulation are: $D = -0.250(5)$ cm^{-1}, $E = 0.044(5)$ cm^{-1} and $g_x = g_y = g_z = 2.000(5)$

In the 5 K spectrum (Figure 3B), the furthest transition (9.11 T) from the center of the spectrum (close to $g = 2.00$ for Mn^{II};[12] 10.18 T at 285 GHz) is associated with the $|5/2,-5/2> \rightarrow |5/2,-3/2>$ transition along the z axis, since $D_{zz} > D_{xx}$ and D_{yy} (with $D_{zz} + D_{xx} + D_{yy} = 0$). This is in agreement with the fact that, at low temperature, only the first Zeeman levels (Ms) levels are populated ($|-5/2>$ and $|-3/2>$). From its field position, the sign and an estimate of the magnitude of D can be obtained. Since this transition is located in the low-field part of the spectrum at low temperature, we infer that the sign of D is negative. Its distance from the central field of the spectrum is $4D/g_z\beta$, implying a D value of 0.27 T or 0.25 cm^{-1} (with $g_z = 2.00$ as a first approximation). The intensity of the transition observed at 9.60 T increases from 5 to 10 K (Figure 3D), in agreement with the Boltzmann population of the Ms levels. Thus, it can be attributed to the $|5/2,-3/2> \rightarrow |5/2,-1/2>$ transition along z. Moreover, this transition is located at the expected field position of $+2D/g_z\beta$ from the $|5/2,-5/2> \rightarrow |5/2,-3/2>$ transition along z, confirming our analysis.

The other 5 K spectrum features are associated with x and y transitions. The 10.98 T and 10.59 T features are associated with the $|5/2,-5/2> \rightarrow |5/2,-3/2>$ and $|5/2,-3/2> \rightarrow |5/2,-1/2>$ transitions along the x axis, respectively. These assignments were confirmed thanks to the temperature effect on the intensity of the transitions. Indeed, the intensity of the first transition of the multiplet decreases on going from 5 to 10 K whereas the second feature increases. The E term can be extracted from the resonance-field difference of these two subsequent x transitions, which corresponds to $(3E - D)/g_x\beta$. This implies an E value of 0.038 cm^{-1}.

The transitions associated with the y axis for the $Ms = -5/2$ and $-3/2$ levels of **1** are observed at 10.47 T and 10.34 T, respectively, which yields a field difference of 0.13 T equal to $-(D + 3E)/g_y\beta$, giving an E value of 0.043 cm^{-1}. This value is similar to the previous one obtained from the x transitions.

Concerning the central feature located at $g = 2.0$ (10.18 T at 285 GHz), it corresponds to the contribution of the $|5/2,-1/2> \rightarrow |5/2,+1/2>$ transitions along the three magnetic axes. At 5 K, the major contribution comes from the y transition since the Ms level $|-1/2>$ is not populated in the x and z directions. On the contrary, at higher temperatures the $|5/2,-1/2> \rightarrow |5/2,+1/2>$ transitions along x, y and z contribute to the central feature. For this reason, this central transition is largely enhanced at 10 K compared to the other transitions.

The absence of observable splitting due to hyperfine interactions in the experimental spectra originates from the large line width of the spectral features. Different mechanisms can contribute to line broadening. In our case, the line width is not temperature-dependent, implying that the major contribution of the broadening comes from dipolar interactions between metallic centers.

As hyperfine interactions are not observable in the experimental data, the spin Hamiltonian of Equation (2) that describes our system under these conditions is simpler than in Equation (1).

$$H = \beta B \cdot g \cdot S + D[S_z^2 - 1/3S(S+1)] + E(S_x^2 - S_y^2) \quad (2)$$

The HF-EPR spectra were simulated using a full-matrix diagonalization procedure of the spin Hamiltonian [Equation (2)].[6a] The best simulation of the experimental spectra

(Figure 3) was obtained using the following spin Hamiltonian parameters: $D = -0.250(5)$ cm^{-1}, $E = 0.044(5)$ cm^{-1} and $g_x = g_y = g_z = 2.000(5)$. These spin-Hamiltonian parameters also simulate successfully the HF-EPR spectra recorded at all temperatures and frequencies.

HF-EPR Spectroscopy of a Magnetically Diluted Powder of [Mn(tButerpy)(N$_3$)$_2$] in Zinc(II)

To experimentally observe the hyperfine interactions for determining the A term, one way is to minimize the line broadening by diluting the paramagnetic centers. A good way to magnetically dilute a paramagnetic center is to incorporate the sample in a diamagnetic host in order to decrease the dipolar interactions. We therefore diluted complex **1** in the corresponding zinc(II) complex at a concentration of approximately 5% by weight of manganese(II).

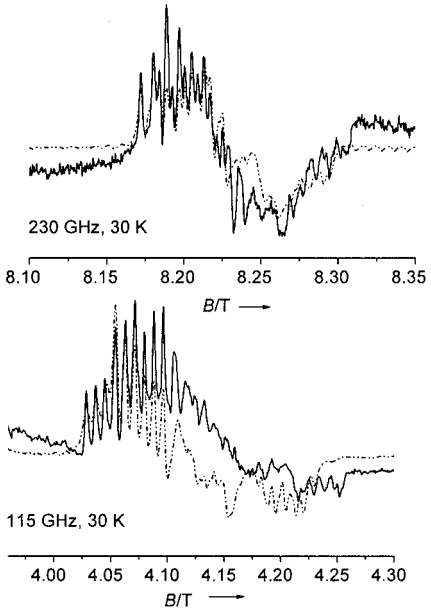

Figure 4. Experimental (bold line) and simulated (dashed line) EPR spectra recorded at 230 and 115 GHz of [Zn(Mn)(*t*Buterpy)(N$_3$)$_2$] at 30 K; the parameters used for the simulation are: $|D| = 0.260(1)$ cm^{-1}, $E = 0.043(1)$ cm^{-1}, $g_x = g_y = 2.001(1)$ $g_z = 2.0005(5)$ and $A_{xx} = A_{yy} = A_{zz} = 77.5$ (5) G

Figure 4 displays the 115 and 230 GHz experimental and simulated EPR spectra of [Zn(Mn)(*t*Buterpy)(N$_3$)$_2$]. As expected, this spectrum is characterized by a unique feature located at $g \approx 2.0$, split into multiple lines corresponding to the $|5/2,-1/2> \rightarrow |5/2,+1/2>$ transition along the three axes x, y and z. Since the two experimental spectra are centered at a g value of around 2.000, the Zeeman interaction is dominant above 4 T. As already observed by Un et al.,[1e] the total width of the spectra increases from 115 to 230 GHz (0.135 and 0.220 T, respectively) and the spectra appear better resolved at low field. Since the exact positions of all of these lines are dependent on the zfs terms (D and E) and g, simulations have been performed to extract the spin Hamiltonian parameters of these spectra.

A full-matrix diagonalization of Equation (1) was performed, and the best simulated spectra using $|D| = 0.260(1)$ cm^{-1}, $E = 0.043(1)$ cm^{-1}, $g_x = g_y = 2.001(1)$, $g_z = 2.0005(5)$ and $A_{xx} = A_{yy} = A_{zz} = 77.5$ (5) G are shown in Figure 4. The sign of D cannot be extracted from the multiplet.

Discussion and Conclusion

In this paper we have described the synthesis and the crystallographic characterization of a mononuclear Mn^{II} complex possessing two terminal azide ligands, [Mn(*t*Buterpy)(N$_3$)$_2$]. Such mononuclear complexes are not common since azide ions have mainly been used for their ability to bridge paramagnetic Mn^{II} centers into dimers, clusters, and polymers.[13] A large number of such compounds have been described in the literature including the dimer [Mn$_2^{II,II}$(μ-N$_3$)$_2$(terpy)$_2$](N$_3$)$_2$].[14]

We performed an HF-EPR study of **1** in order to determine the spin-Hamiltonian parameters of this complex. The experiments were performed in the solid state both on the neat compound and its magnetically diluted form. From the HF-EPR experiments carried out on the neat powder, we extracted the magnitude of g, D and E, as well as the sign of D. The unambiguous determination of the sign of D was possible by recording the spectra at low temperature. In previous HF-EPR studies on mononuclear Mn^{II} complexes, the sign of D was not determined since the experiments were performed at room temperature.[8] The experiments conducted under magnetically diluted conditions allow us to determine the A term and to confirm the value of the other spin-Hamiltonian parameters; the sign of D cannot

Table 2. Electronic characteristics and coordination number of Mn^{II} sites in enzymes

	D [10^{-4} cm^{-1}]	E [10^{-4} cm^{-1}]	A [Gauss]	Coord. number	Ref.
Mn^{2+}-FosA + substrate	2300	200	–	5	[3b]
Mn-SOD *R. capsulatus*	3588	146	86	5	[1e]
Mn-SOD *E. coli*	3548	305	85	5	[1e]
R. capsulatus + azide	720	193	81	6	[1e]
E. Coli + azide	462	91	82	6	[1e]
Mn^{2+}-FosA	600	60	–	6	[3b]
Mn^{2+} concanavaline A	216	23.7	92.5	6	[2d]
Mn^{2+} xylose isomerase	422–450	105.5–112.3	–	6	[4b]

be extracted. Since both sets of parameters are essentially the same, a similar environment for each manganese ion can be postulated in both pure and diluted lattices.

In Table 2, we report the spin-Hamiltonian parameters of several mononuclear Mn^{II} complexes present in different metalloproteins. In all cases the spin-Hamiltonian parameters have been accurately determined from the EPR hyperfine split multiplet of the $|5/2,-1/2> \rightarrow |5/2,+1/2>$ transition using extended spectroscopic techniques such as Q-band EPR, HF-EPR or HF-ENDOR. The coordination number cannot be adequately correlated to A, although such a correlation has already been proposed.[4a,15] On the contrary, a good agreement is observed between the magnitude of D and the coordination number of the Mn^{II} ion. D is larger than 0.2 cm^{-1} for pentacoordinate complexes while it is smaller than 0.1 cm^{-1} for hexacoordinate ones. The D value found for **1** is in good agreement with a pentacoordinate complex. The large E/D value (0.176) reflects the distortions observed in the X-ray structure of complex **1**.

We found similar spin-Hamiltonian parameters to simulate both neat and magnetically diluted powder of **1**. This result shows that the analysis of the HF-EPR spectrum under diluted conditions is sufficient to allow an accurate determination of the electronic parameters of mononuclear Mn^{II} complexes. For the study of manganese sites present in metalloproteins, samples obviously correspond to diluted conditions where only the $|5/2,-1/2> \rightarrow |5/2,+1/2>$ transition can be observed. As shown in Table 2, where all spin-Hamiltonian parameters have been determined using Q-band or HF-EPR spectroscopy, the advantage of increasing the frequency is that the spectra are simpler than X-band spectra. Consistent with this view, our work confirms that HF-EPR spectroscopy permits the resolution of the electronic structure of mononuclear Mn^{II} complexes even for systems with a large D value, making it a promising tool for the study of Mn^{II} compounds, including metalloproteins.

Experimental Section

General: Reagents and solvents were purchased commercially and used as received. ***Caution:*** Both N_3^- and its complexes are potentially explosive; although we have encountered no such problems with complex **1**, it should still be handled with care; further, N_3^- releases explosive HN_3 on contact with acid solution!

Synthesis of [Mn(*t*Buterpy)$(N_3)_2$]: An ethanolic solution (10 mL) of *t*Buterpy (0.055 g, 0.136 mmol) was added, with stirring, to an aqueous solution (2 mL) of $MnCl_2$ (0.017 g, 0.136 mmol). An excess of solid NaN_3 was then added to the yellow solution. The solution was filtered to remove any impurities and the solvents were evaporated to dryness to give a yellow precipitate corresponding to complex **1**. Single crystals of [Mn^{II}(*t*Buterpy)$(N_3)_2$] were grown by slow diffusion of diethyl ether into a concentrated solution of **1** in a mixture of dichloromethane and acetonitrile (1:1). Yield: 0.032 g (22%). $C_{28}H_{38}MnN_9O_{0.5}$ (563): calcd. C 59.67, H 6.80, N 22.37; found C 60.42, H 6.70, N 22.40. IR (KBr): $\tilde{\nu}$ = 2959 (m) cm^{-1}, 2076 (vs), 1607 (s), 1549 (m), 1402 (m), 1364 (m), 1251 (m), 1013 (m), 845 (m).

Synthesis of [Zn(Mn)(*t*Buterpy)$(N_3)_2$]: $[Mn(O_2CCH_3)_2]\cdot 4H_2O$ (0.0032 g, 0.013 mmol) was added with stirring to a methanolic solution (5 mL) of $[Zn(O_2CCH_3)_2]\cdot 2H_2O$ (0.0551 g, 0.25 mmol). A solution of *t*Buterpy (0.1056 g, 0.263 mmol) in 100 mL of methanol was then added to this solution. Finally, an excess of solid NaN_3 was added. The solution was stirred for 1 h until formation of a white precipitate. The solution was filtered and the filtrate was concentrated to dryness to give a yellow precipitate of [Zn(Mn)(*t*Buterpy)$(N_3)_2$]. Yield: 0.045 g (31%).

Crystal-Structure Determination of [Mn(*t*Buterpy)$(N_3)_2$]: Diffraction data were collected with an Enraf-Nonius CAD4 diffractometer. The structures were solved by direct methods and refined using the TEXSAN software package (Single Crystal Structure Analysis Software, version 1.7, molecular structure corporation, 3200 Research Forest Drive, The Woodlands, TX 77381, USA, **1995**). Further details of the data collection and refinement are given in Table 3. CCDC-209520 (**1**) contains the supplementary crystallographic data for this paper. These data can be obtained free of charge at www.ccdc.cam.ac.uk/conts/retrieving.html [or from the Cambridge Crystallographic Data Centre, 12 Union Road, Cambridge CB2 1EZ, UK; Fax: (internat.) + 44-1223-336-033; E-mail: deposit@ccdc.cam.ac.uk].

Physical Measurements: IR spectra were obtained with a Perkin−Elmer Spectrum GX spectrophotometer, piloted by a Dell Optiplex GXa computer. Spectra were recorded with a solid sample at 1% in mass in a pellet of KBr. High-frequency and high-field EPR spectra were recorded with a home-made spectrometer.[16] Gunn diodes operating at 95 GHz and 115 GHz and equipped with a second-, third-, fourth-, and fifth-harmonic generator were used as the radiation source. The magnetic field was produced by a superconducting magnet (0−12 T). The HF-EPR experiments were performed on polycrystalline powder pellets of **1** in order to avoid magnetic orientation of crystals. Diluted samples of **1** were prepared by immobilizing the powder either in KBr or in *n*-icosane mull; identical HF-EPR spectra were obtained in both cases.

Table 3. Principal crystallographic data and parameters of complex **1**

Empirical formula	$C_{27}H_{35}MnN_9$
Formula mass	540.57
Crystal system	monoclinic
Space group	*C*2/*c*
Crystal dimensions [mm]	0.56 × 0.20 × 0.12
a [Å]	22.766(4)
b [Å]	11.718(4)
c [Å]	11.343(2)
β [°]	112.10
V [Å^3]	2804(1)
T [°C]	20
λ [Å]	0.7107
$\rho_{calcd.}$ [g·cm^{-3}]	1.281
Z	4
F(000)	1140
Abs coeff [cm^{-1}]	0.503
No. of reflections collected	10088
No. of independent reflections	3475
No. of observed reflections [$I > 2\sigma(I)$]	1634
No. of refined parameters	183
Largest peak/hole [e·Å^{-3}]	0.51/−0.37
R[a]	0.0628
R_w[b]	0.0902

[a] $R = \Sigma||F_o| - |F_c||/\Sigma|F_o|$. [b] $Rw = [(\Sigma w(|F_o| - |F_c|)^2/\Sigma w(F_o^2)]^{1/2}$.

Acknowledgments

We thank Dr. H. Weihe from the Chemistry Department, University of Copenhagen, Denmark, for the simulation software.

[1] [1a] M. L. Ludwig, A.L. Metzger, K. A. Pattridge, W. C. Stallings, *J. Mol. Biol.* **1991**, *219*, 335−358. [1b] A. L. Schwartz, E. Yakilmaz, C. K. Vance, S. Varthyam, R. L. Koder, A.-F. Miller, *J. Inorg. Biochem.* **2000**, *80*, 247−256. [1c] M. M. Whittaker, J. W. Whittaker, *Biochemistry* **1997**, *36*, 8923−8931. [1d] S. Un, P. Dorlet, G. Voyard, L. C. Tabares, N. Cortez, *J. Am. Chem. Soc.* **2001**, *123*, 10123−10124. [1e] S. Un, L. C. Tabares, N. Cortez, B. Y. Hiraoka, F. Yamakura, *J. Am. Chem. Soc.* **2004**, *126*, 2720−2726.

[2] [2a] A. T. Deacon, T. Gleichmann, A. J. Kalb (Gilboa), J. Price, J. Raftery, G. Brabbrook, J. Yariv, J. R. Helliwell, *J. Chem. Soc., Faraday Trans.* **1997**, *93*, 4305−4312. [2b] Z. Zhang, M. Qian, Q. Huang, Y. Jia, Y. Tang, K. Wang, D. Cui, M. Li, *J. Prot. Chem.* **2001**, *20*, 423. [2c] E. Meirovitch, Z. Luz, A. J. Kalb, *J. Am. Chem. Soc.* **1974**, *96*, 7538−7542. [2d] R. Carmieli, P. Manikanda, A. J. Kalb (Gilboa), D. Goldfard, *J. Am. Chem. Soc.* **2001**, *123*, 8378−8386.

[3] [3a] B. A. Bernat, L. T. Laughlin, R. N. Armstrong, *Biochemistry* **1999**, *38*, 7462−7469. [3b] S. K. Smoukov, J. Telser, B. A. Bernat, C. L. Rife, R. N. Armstrong, B. M. Hoffman, *J. Am. Chem. Soc.* **2002**, *124*, 2318−2326.

[4] [4a] A. K. Whiting, Y. R. Bolt, M. P. Hendrich, L. P. Wackett, L. Que Jr., *Biochemistry* **1996**, *35*, 160−170. [4b] R. Bogumil, R. Kappl, J. Hüttermann, H. Witzel, *Biochemistry* **1997**, *36*, 2345−2352. [4c] L. Requena, S. Bornemann, *Biochem. J.* **1999**, *343*, 185−190.

[5] [5a] C. Buy, G. Girault, J.-L. Zimmermann, *Biochemistry* **1996**, *35*, 9880−9891. [5b] H. Käss, F. MacMillan, B. Ludwig, T. Prisner, *J. Phys. Chem. B* **2000**, *104*, 5362−5371.

[6] [6a] C. J. H. Jacobsen, E. Pedersen, J. Villardsen, H. Weihe, *Inorg. Chem.* **1993**, *32*, 1216−1221. [6b] C. Bucher, E. Duval, J.-M. Barbe, J.-N. Verpeaux, C. Amatore, R. Guilard, L. Le Pape, J.-M. Latour, S. Dahaoui, C. Lecomte, *Inorg. Chem.* **2001**, *40*, 5722−5726. [6c] L. R. Gahan, V. A Grillo, T. W. Hambley, G. R. Hanson, C. J. Hawkins, E. M. Proudfoot, B. Moubaraki, K. S. Murray, D. Wang, *Inorg. Chem.* **1996**, *35*, 1039−1044. [6d] E. Meirovitch, Z. Luz, J. Kalb, *J. Am. Chem. Soc.* **1974**, *96*, 7538−7542. [6e] R. D. Dowsing, J. F. Gibson, *J. Chem. Phys.* **1969**, *50*, 294. [6f] F. E. Mabbs, D. Collison, *Electron Paramagnetic Resonance of Transition Metal Compounds*, Elsevier, Amsterdam, **1992**, vol. 16; and references cited therein.

[7] [7a] R. D. Dowsing, J. F. Gibson, D. M. L. Goodgame, M. Goodgame, P. J. Hayward, *J. Chem. Soc. A* **1969**, 1242−1248. [7b] R. B. Birdy, M. Goodgame, *Inorg. Chim. Acta* **1981**, *50*, 183−187. [7c] G. M. Woltermann, J. R. Wasson, *Inorg. Chem.* **1973**, *12*, 2366−2370. [7d] R. A. Palmer, M. C. L. Yang, J. C. Hempel, *Inorg. Chem.* **1978**, *17*, 1200−1203. [7e] D. Vivien, J. F. Gibson, *J. Chem. Soc., Faraday Trans. 2* **1975**, 1640−1653. [7f] C. A. Kosky, J.-P. Gayda, J. F. Gibson, S. F. Jones, D. J. Williams, *Inorg. Chem.* **1982**, *21*, 3173−3179.

[8] [8a] W. B. Lynch, R.S. Boorse, J. H. Freed, *J. Am. Chem. Soc.* **1993**, *115*, 10909−10915. [8b] R. M. Wood, D. M. Stucker, L. M. Jones, W. B. Lynch, S. K. Misra, J. H. Freed, *Inorg. Chem.* **1999**, *38*, 5384−5388.

[9] Due to the disorder of the *tert*-butyl group and the thickness of the needle-type crystals, we were only able to obtain a structure with a reasonable resolution.

[10] L. S. Erre, G. Micera, E. Garribba, A. Cs. Bényei, *New. J. Chem.* **2000**, *24*, 725−728.

[11] P.-Y. Bu, L. Z. Zhang, L.-C. Li, Y. Dai, P. Cheng, S.-P. Yan, Z.-H. Jiang, D.-Z. Liao, *J. Coord. Chem.* **2002**, *55*, 1263.

[12] A. Abragam, B. Bleaney, in *Electron Paramagnetic Resonance of Transition Ions*, Clarendon Press, Oxford, **1970**.

[13] J. Ribas, A. Escuer, M. Monfort, R. Vicente, R. Cortés, L. Lezama, T. Rojo, *Coord. Chem. Rev.* **1999**, 193−195; J. Ribas, A. Escuer, M. Monfort, R. Vicente, R. Cortés, L. Lezama, T. Rojo, *Coord. Chem. Rev.* **1999**, 1027−1068.

[14] [14a] R. Cortés, J. L. Pizarro, L. Lezama, M. I. Arriortua, T. Rojo, *Inorg. Chem.* **1994**, *33*, 2697−2700. [14b] Z.-H. Zhang, X.-H. Bu, Z.-H. Ma, W.-M. Bu, Y. Tang, Q.-H. Zhao, *Polyhedron* **2000**, *19*, 1559.

[15] J. W. Whittaker, M. M. Whittaker, *J. Am. Chem. Soc.* **1991**, *113*, 5528−5540.

[16] [16a] A.-L. Barra, L.-C. Brunel, J. B. Robert, *Chem. Phys. Lett.* **1990**, *165*, 107. [16b] F. Muller, M. A. Hopkins, N. Coron, M. Grynberg, L.-C. Brunel, G. Martinez, *Rev. Sci. Instrum.* **1989**, *60*, 3681−3684.

Received April 23, 2004
Early View Article
Published Online July 22, 2004

